



# Multi-walled carbon nanotube layer-by-layer coatings with a trilayer structure to reduce foam flammability

Yeon Seok Kim, Rick Davis\*

National Institute of Standards and Technology, Engineering Laboratory, 100 Bureau Drive MS-8665, Gaithersburg, MD 20899-8665, USA

## ARTICLE INFO

### Article history:

Received 3 April 2013

Received in revised form 21 October 2013

Accepted 29 October 2013

Available online 6 November 2013

### Keywords:

Layer-by-layer assembly

Carbon nanotube

Trilayer

Flammability

Polyurethane foam

Cone calorimeter

## ABSTRACT

In order to improve the stability and growth speed of coating, a trilayer (TL) methodology was adapted and resulting film shows high thickness compared to the dimensions of the carbon nanotube. First, the multi-walled carbon nanotubes were functionalized via simple direct amination to be stabilized in the water with positive surface charge. Amine functionalized carbon nanotubes were deposited on polyurethane foam using layer-by-layer assembly with a TL approach. Additional polyethyleneimine layer promote the interaction between carbon nanotube and polymer layers resulting in uniform, durable and thick coating. The  $440 \pm 47$  nm thick 4 TL coatings of polyacrylic acid, polyethyleneimine functionalized multi-walled carbon nanotubes, and polyethyleneimine completely covers the entire internal and external surfaces of the foam. Microscopic images confirm strong polymer/nanotube interaction due to additional polyethyleneimine layer and well dispersed carbon nanotube network on the polyurethane foam surface. The carbon nanotube network created by the layer-by-layer process significantly reduces the flammability of foam (e.g.,  $35 \pm 3\%$ ) reduction in peak heat release rate and prevents pool fire by creating protective layer.

Published by Elsevier B.V.

## 1. Introduction

Layer-by-layer (LbL) assembly has been studied for last two decades as a thin film fabrication technique [1–3]. LbL coatings/thin films are commonly fabricated through alternate deposition of a positively charged layer and negatively charged layer (one pair of positive and negative layers are called a bilayer, BL) [4]. Their characteristics and functional purpose (e.g., oxygen barriers [5] and sensors [6]) are controlled by the fabrication parameters (e.g., pH of solution, solution concentration, and temperature) and the materials that form the coatings (e.g., polymer type) [7–11]. Recently LbL coatings were shown to significantly reduce the flammability of cotton fabrics, polymeric films, and polyurethane foams (PUF) [11–18]. During combustion, the polymer/nanoparticle coatings form a protective residue, which inhibit flame spread and fire growth. Studies have shown polymer only LbL coatings can reduce the flammability of cotton fabrics [16–18]; however, it appears nanoparticles in the assembled coatings can greatly reduce the flammability of PUF. A carbon nanofiber (CNF) and a montmorillonite clay based LbL coatings in previous studies reduced the PUF peak maximum heat release rate (PHRR) PUF by 40% [19,20]. The CNF-based coating naturally grew exponentially due to the inter-diffusion of polyethylenimine (PEI) and poly(acrylic acid) (PAA). The clay-based coating, unlike the CNF-based, has a slow and a linear growth [10], which is not practical for commercialization of this FR technology. However, the growth rate was significantly accelerated by using a using

a trilayer (TL) approach; the clay-based coating thickness was up to  $1 \mu\text{m}$  after 8 TL of deposition [20]. The conventional clay-based LbL coatings utilize electrostatic attraction between the clay platelet and polyelectrolyte, which is a very poor interaction. The TL approach combines the electrostatic attraction and hydrogen bonding by depositing an additional polyelectrolyte layer after clay layer, which helps retain clay in the coating and enables interdiffusion between the two polymer layers.

Since the discovery of carbon nanotubes (CNT) in early 1990, the characteristics of carbon nanotubes (e.g., such as small size and high aspect ratio [21,22], high modulus [23], and high thermal conductivity [24]) have been attractive to enhancing the performance of polymeric materials. Compared to CNFs, which have similar composition and much larger geometry, CNTs have superior physical properties along with at least an order of magnitude higher surface area. Recently, CNTs were deposited via LbL assembly and the resulting films showed excellent property improvement for various applications [25–27]. However, these CNT-based coatings would not be practical as a fire retardant (FR) because the coatings were too thin (less than 100 nm even after 10 BL).

Compared to the previous reports of CNF [19] and clay-based [20] LbL coatings, the MWCNT-based coating have significant challenges stemming from the MWCNT size and surface chemistry that make it difficult to disperse and maintain dispersed in aqueous solutions. Researchers have reported improving MWCNT dispersion, distribution, and stability using non-covalent stabilizing agents (e.g., surfactants [28–30], water-soluble polymers [31–33], and inorganic nanoparticles [34,35]) and have chemically modified the CNTs. Covalent functionalizing is generally

\* Corresponding author. Tel.: +1 3019755901; fax: +1 3019754052.  
E-mail address: [rick.davis@nist.gov](mailto:rick.davis@nist.gov) (R. Davis).



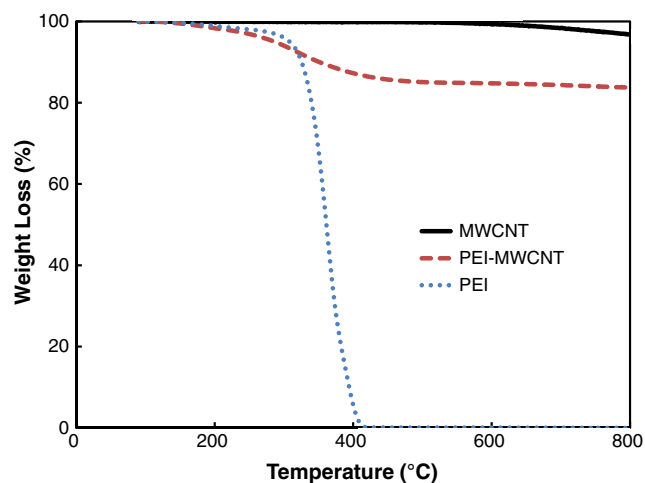


Fig. 2. Thermogravimetric result of pristine MWCNT, PEI-MWCNT, and PEI. The PEI content of PEI-MWCNT was calculated by subtracting PEI-MWCNT from pristine MWCNT.

were easily released from the coating. In an attempt to improve MWCNT stability in water and improve adhesion to the substrate, PEI or sodium deoxycholate surfactant was added to the MWCNT depositing solution. Both approaches failed to be effective, but did show sufficient promise (i.e., longer time for MWCNT to precipitate in the depositing solution) to consider covalently attaching PEI to MWCNT (MWCNT-PEI). The MWCNT-PEI prepared in this study contained 12 mass fraction % PEI (Fig. 2), which was approximately double what was reported by the authors of this process [36]. Presumably our higher PEI content was due to a higher surface area and/or more functional sites on the MWCNT we used in this study. This MWCNT-PEI formed a suspension that remained stable in water for more than a week. The MWCNT-based coated PUFs fabricated using MWCNT-PEI solutions, where a homogenous dark gray color, indicating that using the MWCNT-PEI increased both MWCNT retention and degree of distribution. However, the water wash solutions were still a slight gray color, indicating some unbound MWCNT was still being released.

In a BL coating, the PAA monolayer is deposited onto the MWCNT-PEI monolayer. During the PAA deposition, the PAA solution became gray and the substrate became a lighter gray indicating some of deposited MWCNTs released into the PAA solution. This not only decreases the MWCNT concentration on the substrate, but also restricts PAA deposition by altering the pH value of the solution. After 4BL, the substrate

was a uniform gray color, but the color was significantly lighter than previously reported for CNF-based LbL coating on PUF [19]. SEM images show the MWCNTs are distributed across the substrate, but there are significant amounts of large MWCNT aggregates that appear not to be coated with PAA (Fig. 3). The coating thickness is less than 100 nm after 4BL, which in our experience is not sufficient for FR applications. Rather than focusing on improving MWCNT-PEI and PAA adhesion, the problem of MWCNT-PEI retention was addressed by depositing an additional PEI monolayer between the MWCNT-PEI monolayer and PAA monolayer. This TL approach was previously shown to significantly improve the growth rate of clay-based LbL coatings [20]. Unlike the clay-based TL coating, where PAA was added after clay monolayer, the PEI monolayer was deposited after MWCNT-PEI monolayer. The substrates fabricated using MWCNT-PEI and the TL approach were a uniform black color and had a high concentration of well distributed MWCNTs throughout the entire substrate.

The microstructure of the MWCNT-PEI coating on PUF as a function of the number of TL is shown in the SEM images (Fig. 4). The characteristics of the 1TL (Fig. 4a) and 4BL (Fig. 3) coatings are quite similar; e.g., similar substrate color, high MWCNT distribution, and the presence of MWCNTs that are not covered by polymer. At 2TL, the MWCNTs appear to be mostly covered (Fig. 4b). Above 2TL, the MWCNTs are completely embedded and are very well distributed in the polymer coating (Fig. 4c to e). These coatings have more of a plastic-like look with the MWCNTs not noticeable unless at high magnification or in one of the few tens of micron sized and very sparse aggregates. In less than 5% of the specimens 10 nm  $\pm$  5 nm cracks were observed in the 2TL and greater coatings. Presumably these cracks are formed during drying, but do not appear to negatively impact fire performance.

Cross-section views of 4TL MWCNT-PEI/PUF were taken with the fracture surface in the plane of the image (Fig. 5). The coating is clearly distinguishable from the PUF substrate, which enables measuring the coating thickness. The coating is 440 nm  $\pm$  47 nm thick based on seven measurements taken on each of five different MWCNT-PEI/PUF specimens (value based on 35 measurements). The surfaces in the cross-section views are consistent with those from the surface views in Fig. 4, e.g.; all MWCNT-PEI are embedded in the coating. The surface crack is at least an order of magnitude larger than those observed in Fig. 4 suggesting this crack resulted from the freeze fracture process. The MWCNTs are seen across the entire fracture surface indicating MWCNTs are distributed through the entire depth of the coating as well as across the entire substrate. There are no gaps or pores between the MWCNTs and the polymer coating suggesting strong adhesion. Occasionally a small gap is observed between the coating and the substrate, which is believed to be a side effect of the violent fracturing process. These

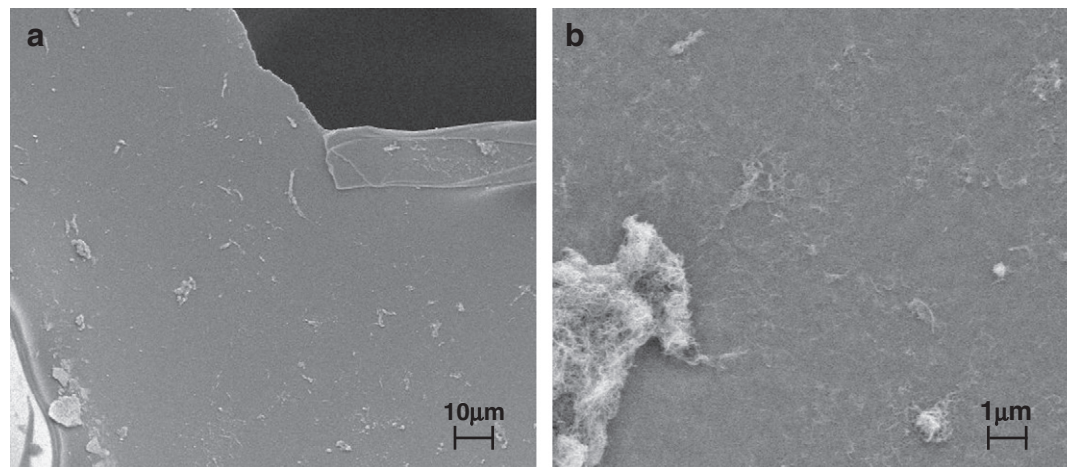
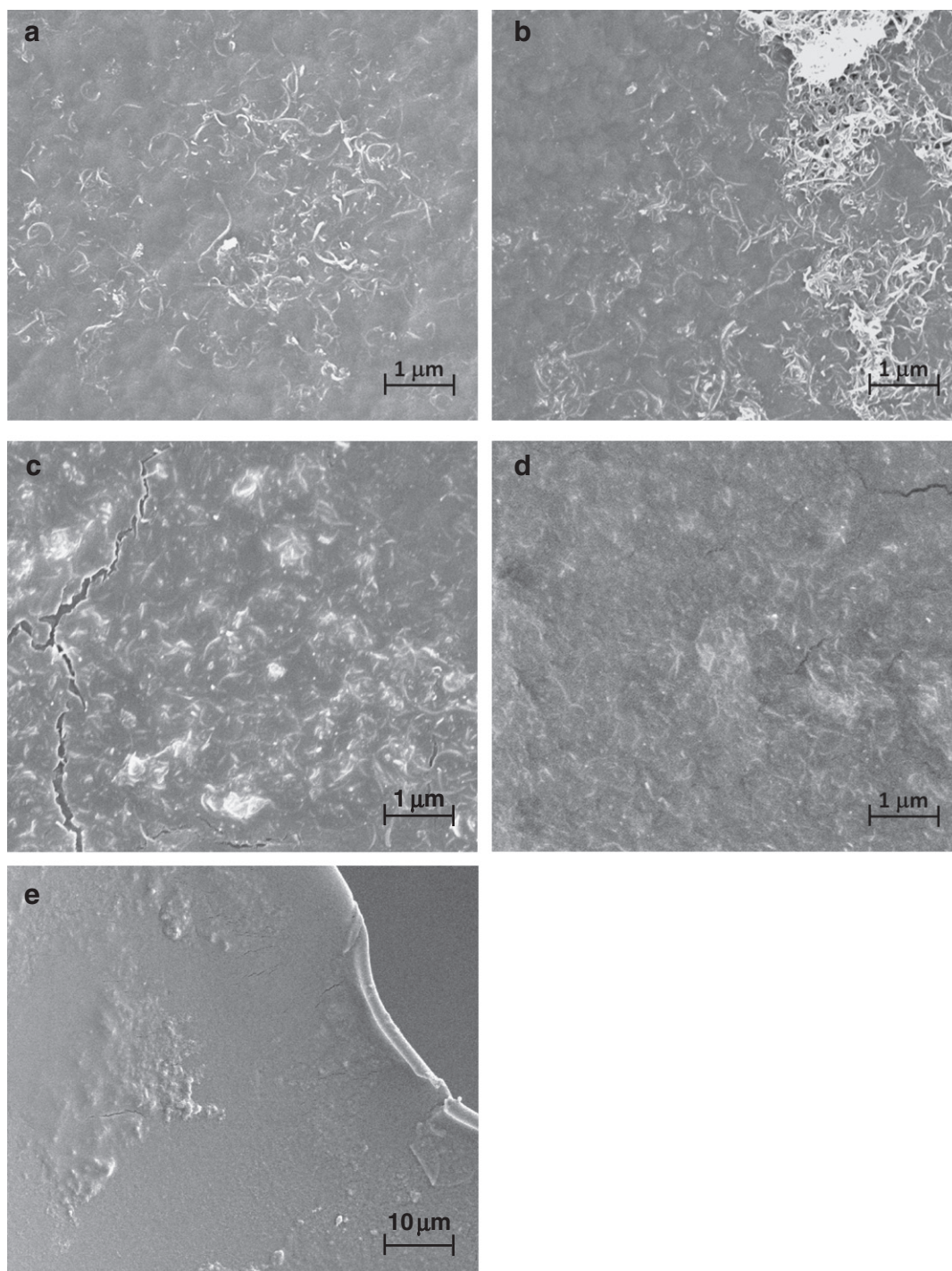


Fig. 3. SEM images of 4BL MWCNT coating at (a) 5000 $\times$  and (b) 100,000 $\times$ . MWCNT well covers the entire surface, but major portion of MWCNT is exposed in the air indicating the weak polymer/MWCNT interaction.



**Fig. 4.** SEM image of (a) 1 TL, (b) 2 TL, (c) 3 TL, (d) 4 TL at 100,000 $\times$ , and (e) 4 TL at 10,000 $\times$ . More MWCNT is embedded into polymer layer due to strong polymer/MWCNT interaction. At 4 TL, all MWCNTs are completely embedded into polymer. Low magnification SEM image shows that the coating surface is very smooth without any exposed MWCNT even within the large aggregates.

gaps were seen in only a few images suggesting the strong adhesion of the coating to the substrate. These observations suggest the coating will be durable during routine stresses experienced by PUF; e.g., compression and release.

MWCNT concentration in the TL coatings was calculated based on TGA and microbalance measurement results. The 4TL coating increased substrate mass by  $(3.4 \pm 0.4)$  mass fraction % and contained  $(51 \pm 1)$  mass fraction % MWCNT. These values are comparable to previously reported CNF-based 4BL PAA/CNF coating on PUF [19], but the MWCNT-PEI 4TL coating is nearly 90 nm thicker. Even though combining PAA

with PEI monolayers will result in exponential growth rate, this cannot explain the thicker MWCNT coating because the MWCNT mass content would be lower than reported for the CNF coating. Therefore, it is assumed the thickness differential is based on nanoparticle packing. MWCNTs and CNFs have a similar density, but MWCNTs are about one order of magnitude smaller. At a given mass there are more MWCNTs than CNFs. The SEM images showed the CNFs occasionally overlap another CNF, but for the most part there is one CNF spanning the depth of the coating with its nearest neighbor several nanometers away. MWCNTs are three dimensionally in contact with several MWCNTs

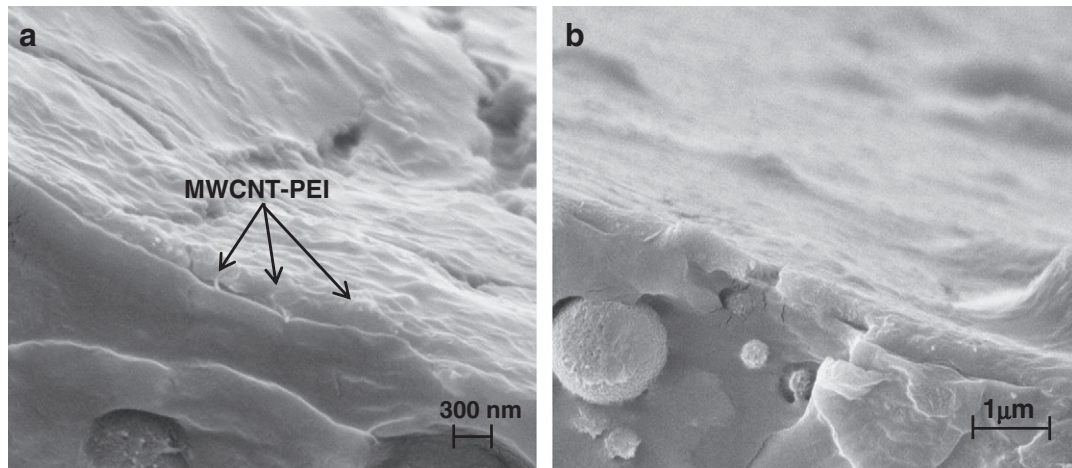


Fig. 5. SEM images of freeze fractured edge of 4 TL PUF at (a) 200,000 $\times$  and (b) 100,000. MWCNTs are well embedded into polymer layer without any void or gap.

(as seen in Figs. 4 and 5). The random direction of the MWCNT deposition may be a factor in the thicker coating.

The MWCNT-PEI TL and previously reported clay-based TL coatings are similar but the underlying mechanism is different. The role of additional PAA monolayer for clay is to promote the deposition of the following PEI monolayer by interacting with clay platelets through hydrogen bonding [20]. For MWCNT-PEI, the PEI monolayer fills the gap between the nanotubes and interacts with PAA monolayer. Even though MWCNTs are flexible and well dispersed, due to the random alignment of MWCNTs there will be voids between the nanotubes, which hinder the PAA deposition and weaken the layer interactions in the BL coating. In the TL system, PEI interacts with the MWCNT-PEI as if it is PEI and penetrates through the MWCNT-PEI monolayer to the PAA (as reported for [20]). This attraction enhances growth, strength monolayer adhesion, and increases MWCNT retention.

### 3.2. MWCNT-PEI/PUF flammability

Cone Calorimetry (Cone) was used to evaluate the flammability of MWCNT/PUF in accordance with ASTM E1474. Cone is a common bench scale test to measure the forced burning behavior of polymers by placing a specimen under the electric heater and igniting it with an electric spark. The Cone data of 4TL MWCNT/PUF and uncoated PUF is provided in Fig. 6 and Table 1. The heat release rate (HRR) curves for MWCNT/PUF and PUF both consist of two peaks. The MWCNT-

PEI coating resulted in a delay to maximum HRR for each peak by  $21 \pm 10\%$  ( $21 \pm 2$  s and  $75 \pm 3$  s as compared to  $34 \pm 2$  s and  $78 \pm 2$  s for MWCNT/PUF). The overall peak maximum HRR (PHRR) for the curve was delayed by  $41$  s  $\pm$   $3$  s and reduced by  $35 \pm 3\%$  ( $620 \pm 26$  kW/m<sup>2</sup> as compared to  $403 \pm 10$  kW/m<sup>2</sup>). The THR and total burn time was also reduced by  $21 \pm 3\%$  and  $25 \pm 3\%$ , respectively. The first peak of MWCNT/PUF is higher than the PUF due to the larger exposed area of MWCNT/PUF and lower heat flux for untreated PUF. During the first peak, PUF completely collapses and forms the pool of combustible compounds. The distance between the top surface of PUF and electric hear increases as the PUF collapses resulting in lowering the heat flux. The MWCNT/PUF maintains its shape so that the exposed area is larger than the PUF. Similar to the CNF-based coating in the previous study, the improvement of fire performance of the MWCNT-PEI/PUF is based on MWCNT network formation, shape retention, and char formation. The lower first peak of the control foam is due to the melting of PUF that increases the distance between heating element of cone and the top surface of PUF resulting in low incident heat flux and HRR values. In a real fire, these coatings are expected to provide a greater improvement in flammability reduction than shown by the Cone, as the MWCNT coatings completely prevent the melt dripping of PUF, which, in a real fire, increases the fire threat of soft furnishing by 35% [40].

### 3.3. Comparison to CNF- and clay-based coatings

All three nanoparticle (CNF, clay, and MWCNT) coatings have distinctly different characteristics. More specifically, the CNF-based coatings are rougher with an appearance more similar to a fibrous network. All of the coatings cover all the PUF surfaces; however, the CNFs tend to deposit as groups rather than individual fibers, which results in regions of high (tens of microns in size) and regions of no (less than a few microns in size) CNFs. The highly aggregated regions contain fibers that are only partially embedded in the polymer coating. The CNF dimension is about one order of magnitude larger than the MWCNTs, which creates a rougher coating surface and larger aggregation of CNFs. Inconsistent coating thickness and large cracks from microscopy images suggest that the coatings may not grow above the reported thickness. In contrast, the MWCNT and clay coatings completely and uniformly cover the entire surface of the PUF with only a few sparsely distributed nanoparticle aggregates. The coatings appear smooth and featureless at lower magnifications. Adding extra polymer layers promotes nanoparticle/polymer interactions and creates a much smoother surface. Even with a different principle for MWCNT and clay as discussed in previous section, the TL approach effectively enhances

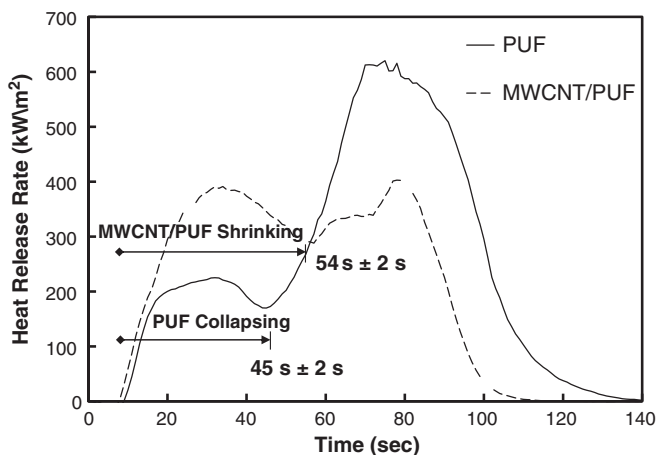


Fig. 6. Heat release rate (HRR) curves of the washed standard PUF and the MWCNT/PUF. The four TL MWCNT coating resulted in 35% reduction in PHRR, 21% reduction in THR, and 25% reduction in total burn time.

**Table 1**

Cone Calorimetry data of the PUF and MWCNT/PUF samples. The approximate  $35 \pm 3\%$  reduction in PHRR and  $21 \pm 3\%$  reduction in THR on PUF resulting from the MWCNT coatings is comparable to the values measured for CNF coatings on PUF ( $40 \pm 3\%$  for PHRR and  $21 \pm 3\%$  for THR, respectively) [19]. All values are reported with  $2\sigma$  standard uncertainty.

	Peak 1		Peak 2		THR (MJ/m <sup>2</sup> )	Residue mass %	Burn time (s)
	HRR (kW/m <sup>2</sup> )	Time (s)	HRR (kW/m <sup>2</sup> )	Time (s)			
PUF	224 ± 12	21 ± 2	620 ± 26	75 ± 3	33 ± 2	2.2 ± 0.1	140 ± 2
MWCNT	391 ± 10	34 ± 2	403 ± 10	78 ± 2	26 ± 1	11.1 ± 0.4	105 ± 2

the polymer/nanoparticle interaction and promotes exponential growth. Strong attraction between the nanoparticle monolayer and polymer monolayers induces higher thickness for both coatings (440 nm for MWCNT and 1000 nm for clay) and a smooth surface.

Even though the physical characteristics of the coatings were quite different, reduction in PUF flammability due to the CNF-based and MWCNT-based coatings were similar. The clay-based coatings exhibit a slightly inferior performance compared to the CNF-based and MWCNT-based coatings. More specifically, CNF-based and MWCNT-based coatings resulted in greater than a  $35\% \pm 3\%$  reduction in PHRR and  $21\% \pm 3\%$  THR, while the clay-based coating showed only a 17% reduction in PHRR and 6% in THR (primarily due to the larger second HRR peak). All three systems are able to form fire protective char layers, which will also prevent melt dripping in a real fire.

#### 4. Conclusion

Trilayer LbL coatings constructed with PEI functionalized MWCNTs are shown to reduce the flammability of PUF. The process described here generates 440 nm thick PAA/MWCNT-PEI/PEI TL coatings containing 51 mass % MWCNTs that are well and uniformly distributed across all of the internal and external surfaces of the porous PUF. Other than isolated/sparsely populated MWCNT aggregates and small surface cracks, the MWCNT-PEI/PUF coatings are smooth and featureless. Critical to this LbL process is using PEI functionalized MWCNTs and depositing a monolayer of PEI between the MWCNT-PEI and PAA layers. This LbL coating significantly reduces the heat release rate, total heat release, and total burn time of the PUF with just four TL (e.g.,  $35\% \pm 6\%$  reduction in PHRR). Compared to FR systems commercially used to reduce PUF flammability and using CNF embedded in the PUF, these functionalized MWCNT-based coatings yield a significantly greater reduction in PUF flammability at a significantly lower additive concentration (e.g., 1.6 mass fraction % MWCNT coating on PUF yields a 20% lower THR than a 20 mass fraction % brominated FR in PUF). The MWCNT-based coatings also prevent the formation of a melt pool of burning foam, which in a real fire scenario, may further reduce the resulting fire threat of burning soft furnishings in residential homes by up to 35%. This research presents another milestone for using LbL to fabricate coatings on foam with a range of nanoparticles and other performance-enhancing additives. These results provide additional evidence that the TL approach can be used with different nanoparticles to effectively enhance the nanoparticle/polymer interactions and the quality of the thin films used for multiple applications outside of fire.

#### References

- [1] G. Decher, in: G. Decher, J.B. Schlenoff (Eds.), *Multilayer Thin Films: Sequential Assembly of Nanocomposite Materials*, Wiley-VCH, Weinheim, Germany, 2003.
- [2] P. Podsiadlo, B.S. Shim, N.A. Kotov, *Coord. Chem. Rev.* 253 (23–24) (2009) 2835.
- [3] P. Bertrand, A. Jonas, A. Laschewsky, R. Legras, *Macromol. Rapid Commun.* 21 (7) (2000) 319.
- [4] G. Decher, *Science* 277 (5330) (1997) 1232.
- [5] M.A. Priolo, D. Gamboa, K.M. Holder, J.C. Grunlan, *Nano Lett.* 10 (12) (2010) 4970.
- [6] P.H.B. Aoki, D. Volpati, A. Riul, W. Caetano, C.J.L. Constantino, *Langmuir* 25 (4) (2009) 2331.
- [7] O. Mermut, C.J. Barrett, *J. Phys. Chem. B* 107 (11) (2003) 2525.
- [8] L. Chang, X.X. Kong, F. Wang, L.Y. Wang, J.C. Shen, *Thin Solid Films* 516 (8) (2008) 2125.
- [9] M.A. Priolo, K.M. Holder, D. Gamboa, J.C. Grunlan, *Langmuir* 27 (19) (2011) 12106.
- [10] Y.H. Yang, F.A. Malek, J.C. Grunlan, *Ind. Eng. Chem. Res.* 49 (18) (2010) 8501.
- [11] Y.C. Li, J. Schulz, J.C. Grunlan, *ACS Appl. Mater. Interfaces* 1 (10) (2009) 2338.
- [12] K. Apaydin, A. Laachachi, V. Ball, M. Jimenez, S. Bourbigot, V. Toniazzo, D. Ruch, *Polym. Degrad. Stab.* 98 (2) (2013) 627.
- [13] Y.C. Li, J. Schulz, S. Mannen, C. Delhom, B. Condon, S. Chang, M. Zammarano, J.C. Grunlan, *ACS Nano* 4 (6) (2010) 3325.
- [14] A. Laachachi, V. Ball, K. Apaydin, V. Toniazzo, D. Ruch, *Langmuir* 27 (22) (2011) 13879.
- [15] G. Laufer, C. Kirkland, A.A. Cain, J.C. Grunlan, *ACS Appl. Mater. Interfaces* 4 (3) (2012) 1643.
- [16] G. Laufer, C. Kirkland, A.B. Morgan, J.C. Grunlan, *Biomacromolecules* 13 (9) (2012) 2843.
- [17] J. Alongi, F. Carosio, G. Malucelli, *Polym. Degrad. Stab.* 97 (9) (2012) 1644.
- [18] F. Carosio, J. Alongi, G. Malucelli, *Carbohydr. Polym.* 88 (4) (2012) 1460.
- [19] Y.S. Kim, R. Davis, A.A. Cain, J.C. Grunlan, *Polymer* 52 (13) (2011) 2847.
- [20] Y.S. Kim, R. Harris, R. Davis, *ACS Macro Lett.* 1 (7) (2012) 820.
- [21] P. Nikolaev, M.J. Bronikowski, R.K. Bradley, F. Rohmund, D.T. Colbert, K.A. Smith, R.E. Smalley, *Chem. Phys. Lett.* 313 (1–2) (1999) 91.
- [22] J.N. Coleman, U. Khan, W.J. Blau, Y.K. Gun'ko, *Carbon* 44 (9) (2006) 1624.
- [23] M.F. Yu, B.S. Files, S. Arepalli, R.S. Ruoff, *Phys. Rev. Lett.* 84 (24) (2000) 5552.
- [24] C.H. Yu, L. Shi, Z. Yao, D.Y. Li, A. Majumdar, *Nano Lett.* 5 (9) (2005) 1842.
- [25] S.W. Lee, B.-S. Kim, S. Chen, Y. Shao-Horn, P.T. Hammond, *J. Am. Chem. Soc.* 131 (2) (2008) 671.
- [26] M.N. Hyder, S.W. Lee, F.C. Cebeci, D.J. Schmidt, Y. Shao-Horn, P.T. Hammond, *ACS Nano* 5 (11) (2011) 8552.
- [27] S.W. Lee, J. Kim, S. Chen, P.T. Hammond, Y. Shao-Horn, *ACS Nano* 4 (7) (2010) 3889.
- [28] C. Fantini, J. Cassimiro, V.S.T. Peressinotto, F. Plentz, A.G. Souza, C.A. Furtado, A.P. Santos, *Chem. Phys. Lett.* 473 (1–3) (2009) 96.
- [29] N. Grossiord, J. Loos, O. Regev, C.E. Koning, *Chem. Mater.* 18 (5) (2006) 1089.
- [30] V.C. Moore, M.S. Strano, E.H. Haroz, R.H. Hauge, R.E. Smalley, J. Schmidt, Y. Talmon, *Nano Lett.* 3 (10) (2003) 1379.
- [31] C. Yu, Y.S. Kim, D. Kim, J.C. Grunlan, *Nano Lett.* 8 (12) (2008) 4428.
- [32] J.H. Zou, L.W. Liu, H. Chen, S.I. Khondaker, R.D. McCullough, Q. Huo, L. Zhai, *Adv. Mater.* 20 (11) (2008) 2055.
- [33] Y.K. Kang, O.S. Lee, P. Deria, S.H. Kim, T.H. Park, D.A. Bonnell, J.G. Saven, M.J. Therien, *Nano Lett.* 9 (4) (2009) 1414.
- [34] L. Liu, J.C. Grunlan, *Adv. Funct. Mater.* 17 (14) (2007) 2343.
- [35] J. Zhu, M. Yudasaka, M.F. Zhang, S. Iijima, *J. Phys. Chem. B* 108 (31) (2004) 11317.
- [36] K.S. Liao, A. Wan, J.D. Batteas, D.E. Bergbreiter, *Langmuir* 24 (8) (2008) 4245.
- [37] Certain commercial equipment, instruments or materials are identified in this paper in order to specify the experimental procedure adequately. Such identification is not intended to imply recommendation or endorsement by the National Institute of Standards and Technology, nor is it intended to imply that the materials or equipment identified are necessarily the best available for this purpose.
- [38] The policy of NIST is to use metric units of measurement in all its publications, and to provide statements of uncertainty for all original measurements. In this document however, data from organizations outside NIST are shown, which may include measurements in non-metric units or measurements without uncertainty statements.
- [39] Y.H. Yang, M. Haile, Y.T. Park, F.A. Malek, J.C. Grunlan, *Macromolecules* 44 (6) (2011) 1450.
- [40] W.M. Pitts, G. Hasapis, P. Macatangga, Eastern States Section Meeting of the Combustion Institute, College Park, Maryland, 2009.